

Utilizing Industrial By-Products in Autoclaved Aerated Concrete: A Sustainable Approach

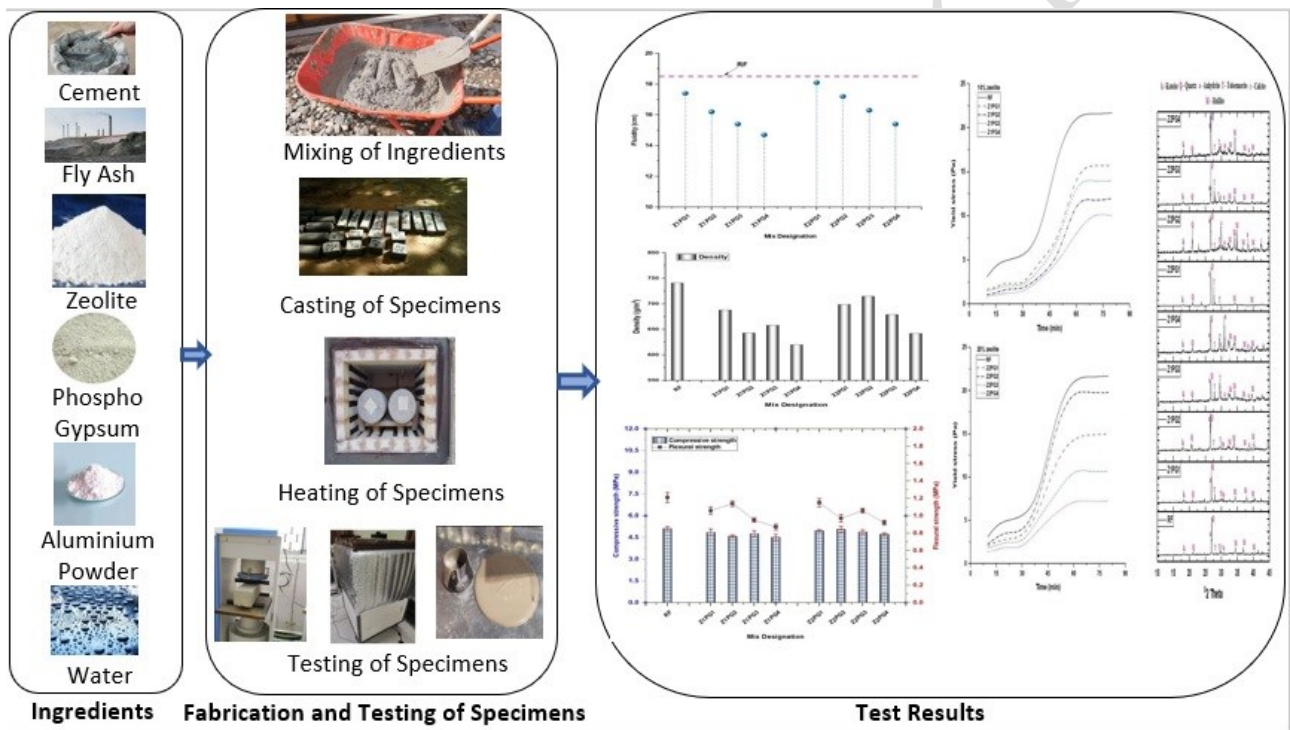
Jagadheeswari R^{1*} and Sumathy SR²

^{1*}Department of Civil Engineering, K Ramakrishnan College of Technology, Trichy - 621112, Tamilnadu, India (sivag616@gmail.com)

²Department of Civil Engineering, Alagappa Chettiar Government College of Engineering and Technology, Karaikudi - 630003, Tamilnadu, India (sr.sumathy5@gmail.com)

Corresponding author: Jagadheeswari R., email: sivag616@gmail.com

Graphical Abstract



Abstract

The feasibility of utilizing natural zeolite (NZ), phosphogypsum (PG), and aluminium (Al) powder (AP) as replacements for fly ash in autoclaved aerated concrete (AAC) is assessed in this research. This study examines the influence of NZ, PG and AP on AAC's fresh state properties, mechanical behavior, and thermal characteristics. Gas foaming properties were analyzed using X-ray diffraction (XRD) and Fourier Transform Infrared Spectroscopy (FTIR). Results show that natural zeolite and aluminum powder have acceptable foaming properties that contribute to AAC's porosity and lightness when combined with phosphogypsum. The optimal dosage of PG, along with 10% and 20% zeolite and aluminum powder, enhances AAC performance through a synergistic effect. PG substitution for fly ash reduced density and increased the pH of the AAC slurry,

21 affecting foam generation. Incorporation of PG potentially reduced workability due to its smaller
22 particle size and larger surface area. Despite this, NZ, PG, and AP combinations resulted in AAC
23 with satisfactory strength and flexural properties. AAC with phosphogypsum showed good
24 strength, density, and thermal conductivity, though thermal conductivity was highest in control
25 AAC. This study demonstrates these materials' potential to meet AAC's construction requirements
26 economically and efficiently dispose of phosphogypsum. Future research should explore other
27 material combinations and their impacts on AAC, supporting sustainable construction and resource
28 management.

29 Keywords: AAC, natural zeolite, phosphogypsum, aluminium powder, strength, foaming property,
30 microstructure

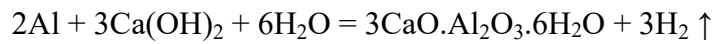
31

32 **1. Introduction**

33 Buildings' total carbon emissions and energy use during their lifetimes are rising due to
34 urbanisation (González et al., 2022). Greenhouse gas emissions can be lowered and the
35 environment protected with the help of energy-efficient construction. It is crucial to advance and
36 popularise carbon-neutral and energy-efficient construction supplies. AAC has more potential for
37 use in the background of universal efforts to encourage construction energy savings and decrease
38 carbon dioxide emissions. Recently, interest has risen in the use and improvement of insulating
39 materials for buildings that condense energy utilization (Tian et al., 2016; Yang et al., 2021;
40 Falliano et al., 2022). Autoclaved aerated concrete (AAC) is a lightweight, porous construction
41 element that can bear significant loads and offers superior insulating properties. AAC has been
42 suggested as a means of improving energy efficiency (Kadhim et al., 2020; Wang et al., 2021)
43 could be a possible solution, and the product reveals small bulk density, good thermal insulation
44 and fire resistance, which can be possibly applied in non-load-bearing structures and as thermal
45 insulation materials for walls in buildings (Trindade et al., 2021; Xu et al. 2021; Qian and Hu
46 2023). Due to their beneficial effects on efficiently harnessing seismic loads, lightweight materials
47 have seen widespread application in recent years (Seddighi et al., 2021). Its density can range from
48 300 to 1800 kg/m³ but is typically 400 to 600 kg/m³ (Zhai et al., 2018). Its structure comprises 60-
49 80% non-connected air pores, which are liable to the density class. Typically, siliceous materials
50 like quartz powder or fly ash and calcareous raw materials like lime and cement, laterally with
51 supplements like foaming agents and water, are autoclaved at temperatures considerably more
52 significant than 100°C in a pressurised, steam-heated environment to create AAC (Schreiner et al.,
53 2018; Natarajan et al., 2021). Acquiring insulating materials for strong and lightweight buildings
54 has always been an objective and a course of action.

55 For this reason, the sector's goal has been extended to produce AAC with greater
56 compressive strength within a given range of density oscillation. Due to its high porosity, the pore
57 structure is a significant determinant of AAC's dry density and compressive strength. Pore structure
58 analysis has emerged as a fundamental topic in concrete materials science (Kumar et al., 2024).
59 AAC's pore structure is comprised mainly of the porosity, number of holes, average pore size, and
60 hole shape component of its pores (Zhang et al., 2023). The mechanical attributes of cement-based
61 materials are closely related to their degree of porosity (Revilla et al., 2021; Loginova et al., 2023).
62 As the porosity of AAC increases, its compressive strength drops dramatically (He et al., 2019).
63 Improved indoor comfort is possible thanks to AAC due to the material's porous properties, high
64 heat preservation, and sound insulation abilities (Qu and Zhao 2017; Liu et al., 2020). The trend has
65 shifted even more towards using industrial by-products to make high-performance AAC. This
66 refers to AAC that maintains its volume, is mechanically robust, and provides excellent thermal
67 insulation (El-Didamony et al., 2019). The fact that fly ash, iron tailings, zinc tailings, and sludge
68 can all be utilised in the production of AAC demonstrates a significant opportunity for improving
69 the current rate of solid waste utilisation (Serhat et al., 2014; Walczak et al., 2015; Suchorab et al.,
70 2016; Miao et al., 2023). Solid wastes made AAC, including calcium carbide slag, gold tailings,
71 and silica fume (Cai et al., 2018; Li et al., 2019; Zhao et al., 2020). This strategy can considerably
72 reduce the price of finished products while still being environmentally friendly and sustainable
73 (Guo and Zhang, 2020). Cementitious materials, such as siliceous and calcareous, comprise the
74 bulk of AAC's raw materials. Classic examples of siliceous minerals include quartz sand and silica
75 sand, which typically have SiO₂ concentrations above 90%.

76 AAC's thermal insulation qualities are superior to regular concrete's, and its density is
77 significantly lower (Ma et al., 2016; Yuan et al., 2017; Asadi et al., 2018). The economic viability
78 of AAC products is constrained by characteristics such as their fragility and lack of mechanical
79 strength (Koudelka et al., 2015; Cong et al., 2016; Johnson et al., 2021). AAC's widespread
80 application in buildings may be traced back to the rise of the "carbon neutralisation" development
81 aim in recent years, which many countries have suggested. Insufficient mechanical characteristics,
82 especially flexure, have been identified as a significant source of AAC non-compliance through
83 preceding investigations publicizing that breakage, cracking, and frost failure are expected during
84 the manufacturing, transportation, and service phases of AAC products (Huang et al., 2022). While
85 cement hydration releases calcium hydroxide, adding aluminium powder to cement-based products
86 stimulates a chemical interaction between the powder and water, producing hydrogen gas and
87 forming porous interior structures (Ahmed et al., 2024). The aluminium powder-cement paste
88 chemical reaction is shown as: (Singh et al., 2020; Wang et al., 2023)



89 Cellular holes between 0.1 and 1.0 mm in size have been reported to be produced in the
90 literature during this chemical process. Consequently, cement-based products with a density of 300-
91 1,800 kg/m³ can be made significantly lighter by adding aluminium powder (Ahmed et al., 2022).
92 Because of this, there have been a lot of inquiries to emphasise the crucial role that aluminium
93 particles' integration into an insulating polymer plays in enhancing the material's mechanical,
94 tribological, thermal, and electrical properties (Zhang et al., 2022). Mechanical, tribological, and
95 electric properties of mixtures were investigated after a novel composite material was produced by
96 filling aluminium powder in acrylonitrile butadiene styrene. A larger powder loading of aluminium
97 filler was shown to have a pronounced effect on the impact, tensile, and flexure of the matrix, as
98 demonstrated by their experiments (Laad and Jatti 2015). A different investigation found that
99 ageing aluminium powder composites improved their resistance to heat, ozone, and gamma
100 radiation. To properly understand cement-based materials' features that combine pore formation
101 components, it's essential to conduct more microscale research to analyse the connection between
102 porous structures and hardened properties. Very porous cement-based materials' mechanical
103 characteristics and longevity are subpar (Li et al., 2015; Kim et al., 2018).
104

105 Industrial waste material phosphogypsum (PG) is produced during the wet production of
106 phosphoric acid. For every ton of phosphoric acid produced, about 5 tons of PG are by-products
107 (Rashad 2017). Approximately 85 percent of all PG is frequently discarded in gigantic mounds
108 without being handled. This leaves it vulnerable to occupying a large amount of land through the
109 progression of weathering and inflicting substantial damage to the natural world, especially along
110 the coast (Zhao et al., 2023). Consequently, several nations have studied PG disposal alternatives in
111 response to widespread resentment. An alternative to the location where waste is disposed of can be
112 achieved by using PG as a binder in civil building activities (Qiao et al., 2020). Recently, much
113 emphasis has been placed on PG's potential as a versatile raw material in the food industry. In the
114 cement industry, PG has been employed as a setting regulator instead of natural gypsum, paving an
115 efficient way to save money (Li et al., 2020). The practice of natural gypsum in setting regulator
116 applications has been replaced mainly by using PG in the cement and gypsum industries. Because
117 of radioactive concerns, PG is not widely adopted in the building business. However, this problem
118 may be overcome by limiting the quantity of PG included in building materials. According to the
119 studies, this would result in radioactivity control that was entirely risk-free for the construction
120 industry (Campos et al., 2017). Because of the rising amount of garbage being produced, it is
121 imperative that these waste materials, in addition to PG, be put to use to prevent the rapid
122 deterioration of the environment (Chen et al., 2021). Ordinary Portland cement, oilwell cement,

123 calcium sulfoaluminate cement, and magnesium phosphate cement are some of the types of cement
124 that make extensive use of PG (Aminul et al., 2020; Mohammadi et al., 2020; Rosales et al. 2020;
125 Reddy et al., 2022; Nambiar et al., 2023). Impurities soluble in phosphoric acid can extend the time
126 needed for the setting process and lower the water-to-binder ratio (Holanda et al., 2017). These
127 impurities have the potential to transform into phases that are insoluble in some types of cement
128 that have a high aluminium content.

129 **Zeolite, a naturally occurring aluminosilicate, offers unique properties that enhance the**
130 **performance of AAC. Its high silica and alumina content makes it a suitable replacement for**
131 **traditional binders like fly ash, contributing to the pozzolanic reaction, which enhances the**
132 **strength and durability of AAC. Additionally, zeolite's porous structure improves the thermal**
133 **insulation properties of AAC, making it an ideal candidate for energy-efficient building**
134 **materials (Rahman et al., 2021). Studies have shown that the inclusion of natural zeolite in**
135 **concrete mixtures can lead to improved compressive strength and long-term stability, as well**
136 **as reduced autoclaving time due to accelerated hydration processes (Shekarchi et al., 2023).**
137 **Moreover, the environmental benefits of using zeolite in AAC are considerable. By reducing**
138 **the reliance on energy-intensive materials like Portland cement, the carbon footprint of AAC**
139 **production is lowered, aligning with sustainable construction practices. Zeolite's ability to**
140 **absorb and neutralize harmful chemicals also adds to its eco-friendly profile, making AAC**
141 **with zeolite a promising material for future green building projects (Alexa-Stratulat et al,**
142 **2023).****2. Research Significance**

143 Although it has been shown through a series of tests that aluminium powder may be carried
144 out to form porous structures in cement-based materials, the outcomes of mixing the two materials
145 and lags in defining the mechanism of their interface, this study focused on the exploitation of
146 phosphogypsum, aluminium powder, and natural zeolite together to develop a better, more durable,
147 and lighter-weight concrete. Regarding the manufacturing of AAC, the aerating agent is the most
148 expensive component. Pure aluminium (Al) powder is the preferred aerating agent for this
149 application's production of lightweight AAC. The primary goal was to determine whether or not the
150 addition of natural zeolite and phosphogypsum could be employed to produce AAC that exhibited
151 higher mechanical performance. When making AAC for testing purposes, different proportions of
152 phosphogypsum and two standard concentrations of zeolite (10% and 20%, respectively) were
153 added to the mixes by the ratios of commercially available AAC.

154 **3. Experimental programs**

155 **3.1 Materials**

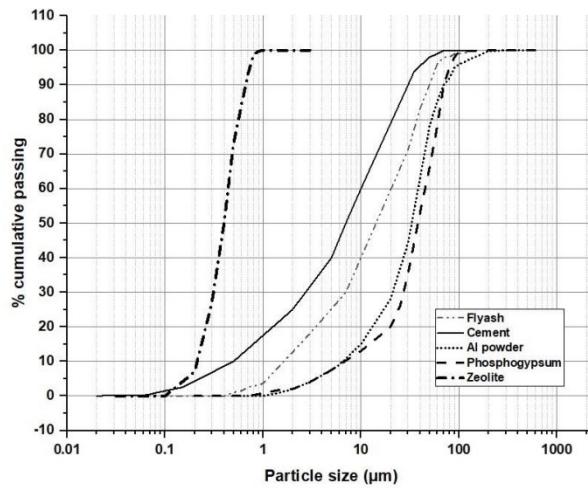


Fig. 1 PSD curves of raw materials

156

157

158 Cement, fly ash, zeolite, lime, phosphogypsum, and aluminium powder were all purchased
 159 from Astrra Chemicals in Tamil Nadu, India, to prepare AAC samples. Each ingredient is
 160 essentially intended to create AAC and satisfy the necessary standards. Ordinary Portland cement
 161 with a grade of 53 is the type of cement employed in manufacturing concrete mixes. According to
 162 IS code 12269-1987, the fineness of the cement shall be more excellent than 225 m²/kg, and the
 163 soundness should be at least 10 mm and 0.8% for Le Chatellier expansion and Autoclave
 164 expansion, respectively. In addition, aluminium powder is utilized as the expanding agent to
 165 increase the slurry's capacity while lowering its density. Table 1 presents the oxide composition of
 166 the raw materials as tested in lab, while Fig. 1 illustrates their particle size distribution curves.

167

Table 1 Percentage of Oxide composition of raw materials

Composition	Cement	Lime	Flyash	NZ	PG	AP
SiO ₂	26.01	1.2	58.22	63.87	3.66	0.1
CaO	53.6	89.1	3.28	2.37	32.31	0.1
SO ₃	2.77	2.2	0.28	-	41.94	-
Al / Al ₂ O ₃	8.54	0.4	28.31	11.47	0.23	99.5
MgO	0.35	0.7	1.14	1.01	0.03	0.1
MnO	0.13	-	-	-	-	-
K ₂ O	0.9	0.1	0.41	0.94	0.02	-
TiO ₂	0.42	-	1.01	-	-	-
P ₂ O ₅	0.17	-	-	-	0.45	-
Na ₂ O	0.18	1.1	0.62	6.81	0.02	0.1
Fe ₂ O ₃	4.09	0.3	3.76	0.22	0.2	0.1
LOI	2.7	3.7	2.97	11.97	21.14	-

168

169 3.2 Sample preparation

170 In this experiment, the constituents used were lime, cement, fly ash, zeolite,
171 phosphogypsum, and water. The ratios of cement, lime, aluminum powder, and water were kept
172 constant during the mixing process. The mixture has been finely pulverized, and the slurries have
173 been mixed at room temperature for sixty seconds. Then, the slurry was blended with aluminium
174 powder while stirred for thirty seconds. Slurries were poured into steel moulds of various sizes (100
175 mm by 100 mm by 100 mm) and then maintained in a steam curing chamber with a continuous
176 temperature of 600 °C to finish the curing process. After removing the portion that had expanded
177 out of the steel mould, demold the remaining material to obtain samples with dimensions of 100
178 millimetres on each side, 100 millimetres in length, and 100 millimetres in height.

179 At last, the sample that has been demoulded is placed inside an autoclave for eight hours at
180 a temperature of 2,000 degrees Celsius and a pressure of two megapascals. Samples were prepared
181 to assess the impact of various replacements on the characteristics of slurry and AAC.
182 Phosphogypsum was used in place of fly ash at percentages of 0%, 5%, 10%, 15%, and 20% by
183 weight, respectively. In addition, a consistent cement substitution of 10% to 20% zeolite is utilized
184 across the board in all mixes. Powdered aluminium is added in an amount equal to 0.5% of the
185 overall mass of the binder. The goal of the Z1PG1–Z1PG4 samples was to see how different
186 amounts of PG affected the AAC's functional characteristics. In contrast, the Z2PG1–Z2PG4
187 samples contained 20% zeolite as a consistent replacement. No alternatives exist in the reference
188 mix (RF), such as zeolite and phosphogypsum. Table 2 displays the mix proportions and the water-
189 solid ratio (w/s). The selection of component ranges in Table 2 was based on a combination of
190 preliminary experiments, previous literature, and the need to maintain optimal properties of the
191 concrete mix. Specifically, the maximum inclusion of phosphogypsum was limited to 20%, to avoid
192 potential adverse effects on compressive strength and workability, which can occur at higher
193 concentrations. Studies have shown that higher ratios of phosphogypsum can negatively impact the
194 mechanical properties of concrete (Arunprathap et al., 2020; Murali & Azab, 2023).

195 **Table 2 Mix proportion of developed samples**

Mix Id	Cement in %	Lime in %	Flyash in %	Zeolite in %	Phospho-gypsum in %	Al powder in %	w/s
RF	10	15	75	0	0	0.5	0.55
Z1PG1	10	15	60	10	5	0.5	
Z1PG2	10	15	55	10	10	0.5	
Z1PG3	10	15	50	10	15	0.5	

Z1PG4	10	15	45	10	20	0.5
Z2PG1	10	15	50	20	5	0.5
Z2PG2	10	15	45	20	10	0.5
Z2PG3	10	15	40	20	15	0.5
Z2PG4	10	15	35	20	20	0.5

196 **3.3 Characterizations and tests**

197 3.3.1 Raw materials

198 To identify the individual chemical components of raw materials, an X-ray fluorescence
 199 (XRF) analyzer was utilized. Quantification was done on the particle size distributions of cement,
 200 fly ash, zeolite, powdered graphite, and powdered aluminium.

201 3.3.2 Properties of slurry

202 The gas-foaming rate was determined by monitoring the slurry volume measurement in a
 203 measuring cylinder that had a capacity of 250 ml and had been stuffed with 100 ml of initial slurry
 204 once every 10 minutes until the slurry stopped growing in volume. The readings of PG's pH were
 205 determined as per ASTM C471M-20, and the pH/ion meter was used to develop the determinations.
 206 Before conducting the tests, powder samples were made in agreement with Table 2 (but without
 207 adding Al powder or water). The slurry was finally ready for use after thoroughly combining the
 208 powder samples and water for ten minutes at a w/s ratio of 0.55. After filtering the slurry to acquire
 209 the filtrate liquid, a pH test was carried out on the product of the extraction of liquid from the
 210 filtering process.

211 3.3.3 Fresh state

212 First, the paste was put into the mould until it reached a height equal to two-thirds of the
 213 height of the mould, and then the mould was tamped 15 times. Next, the paste was poured into the
 214 mould until it reached a height 20 millimetres higher than the mould, which was tamped ten more
 215 times. Following the completion of the tamping process, the formwork was removed. The yield
 216 stress was calculated through a rheometer at a temperature of $27\pm 20^{\circ}\text{C}$. One millilitre of freshly
 217 made AAC paste was placed between two parallel titanium plates with a diameter of 35 mm and a
 218 spacing of 1.1 mm. During the first minute of the experiment, a constant shear rate of 0.5 s^{-1} was
 219 applied to the paste to overcome the initial inertia of the rheometer and break up any
 220 agglomerations that had formed due to the hydration process. Following this, the shear rate
 221 decreased linearly from 0.5 to 0.08 s^{-1} over three minutes, with a reduction step of 0.004 s^{-1} , the
 222 smallest measurable value using the rheometer. According to Pinilla et al. (2014), the rheological
 223 behaviour of aerated cement paste can be modelled using the Bingham model. According to the

224 Bingham model, the equation that describes the relationship between shear stress and shear rate is
225 as follows:

$$226 \quad \tau = \tau_0 + \mu \quad (1)$$

227 Where τ_0 and μ represent the yield stress and viscosity of the fresh paste, respectively,
228 Equation (2) was used to predict the yield stress of the AAC pastes by fitting it to the experimental
229 data obtained from the σ vs. $\dot{\gamma}$ curve. To determine the volume expansion capacity of the AAC, 40 ml
230 of fresh AAC paste was poured into a 100 ml measuring cylinder and stored in an environmental
231 chamber at the same pre-curing temperature and relative humidity as the AAC cube samples. These
232 conditions were 550 degrees Fahrenheit and 98% relative humidity. Every five minutes, the size of
233 the paste was measured and recorded until there was no longer any change. The following equation
234 was used to calculate the volume expansion, denoted by V_t (in ml) at time t :

$$235 \quad \Delta V_t = V_t - V_0 \quad (2)$$

236 Where V_t is the paste volume at time t in ml, and V_0 is the initial paste volume (40 ml). It is
237 vital to remember that the measurement method, particularly the mould's base area chosen to
238 estimate the volume expansion capacity, might have a consequence on the results.

239 3.3.4 Mechanical behavior of AAC

240 The ASTM C1693-11 standard measured the AAC samples' bulk densities. For compressive
241 and flexural strength tests, specimens with overall dimensions of 100 mm x 100 mm x 100 mm and
242 50 mm x 50 mm x 200 mm were constructed. The samples were put into an oven preheated to 600
243 degrees Celsius for one full day to condition them. Afterwards, they were detached from the oven
244 and allowed to relax for 120 minutes before the tests. Evaluation was done on three samples of each
245 composition and pure AAC.

246 3.3.5 Thermal conductivity

247 The developed slurry was set into the mould with dimensions of 70.7 mm by 70.7 mm by
248 70.7 mm, and the extra part that extended beyond the part of the mould where it was supposed to be
249 was chopped off. After the cubes were obtained, they were positioned in the autoclave to undergo
250 the curing process. After the time in the autoclave had elapsed, the cubes were removed and baked
251 at 105 degrees Celsius for three days.

252 3.3.6 Microstructural characterization

253 X-ray diffraction was utilized as the analysis method to study the crystalline phases present
254 in AAC. The XRD tests were executed with the assistance of an XPert Pro PANalytical
255 diffractometer, and the patterns were captured at two different angles. FTIR examinations were
256 carried out to obtain the spectral curves of AACs. The curves were acquired using the Shimadzu IR

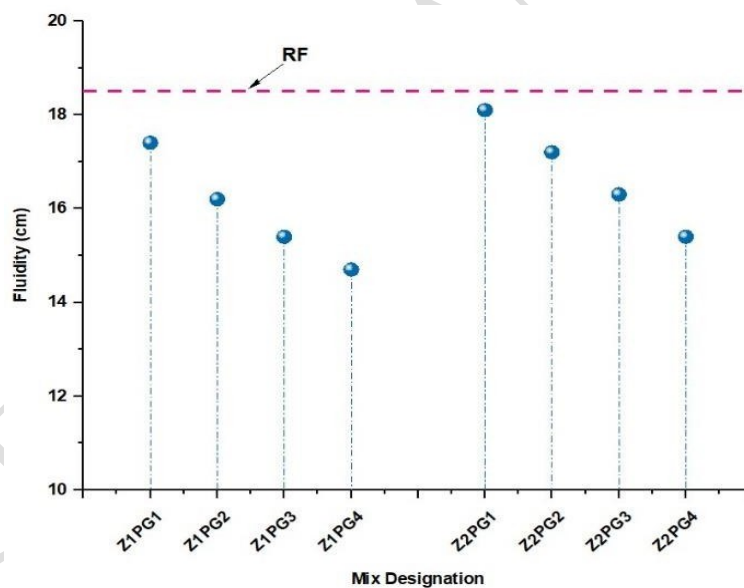
257 Tracer apparatus at a wavelength ranging from 400 to 4500 cm^{-1} utilizing the KBr pellet approach.
258 After the AAC samples were ground into a powder, about one milligram of the powdered AAC
259 samples was combined with 99% potassium bromide (KBr). After that, the mixture is pelletized by
260 creating a homogenous mixture, which leads to the development of crystalline pellets with a hazy
261 appearance.

262 4. Results and Discussions

263 4.1 Fresh state behaviour

264 4.1.1 Fluidity

265 The fluidity of the slurry defines the expansion behaviour and gas foaming capacity of the
266 AAC mixes. This is accomplished through the uniform development of pores in the AAC. As
267 shown in Fig. 2, the fluidity of the AAC mixes became less manageable as the proportion of
268 existing PG additives in the mixture increased. It is readily apparent that the control AAC can
269 achieve better workability. It was revealed that the fluidity of the AAC mix, including 10% New
270 Zealand wool and 20% polypropylene glycol, was 20.5% less than the fluidity of the control mix,
271 indicating that the viscosity of the AAC mixes had grown.

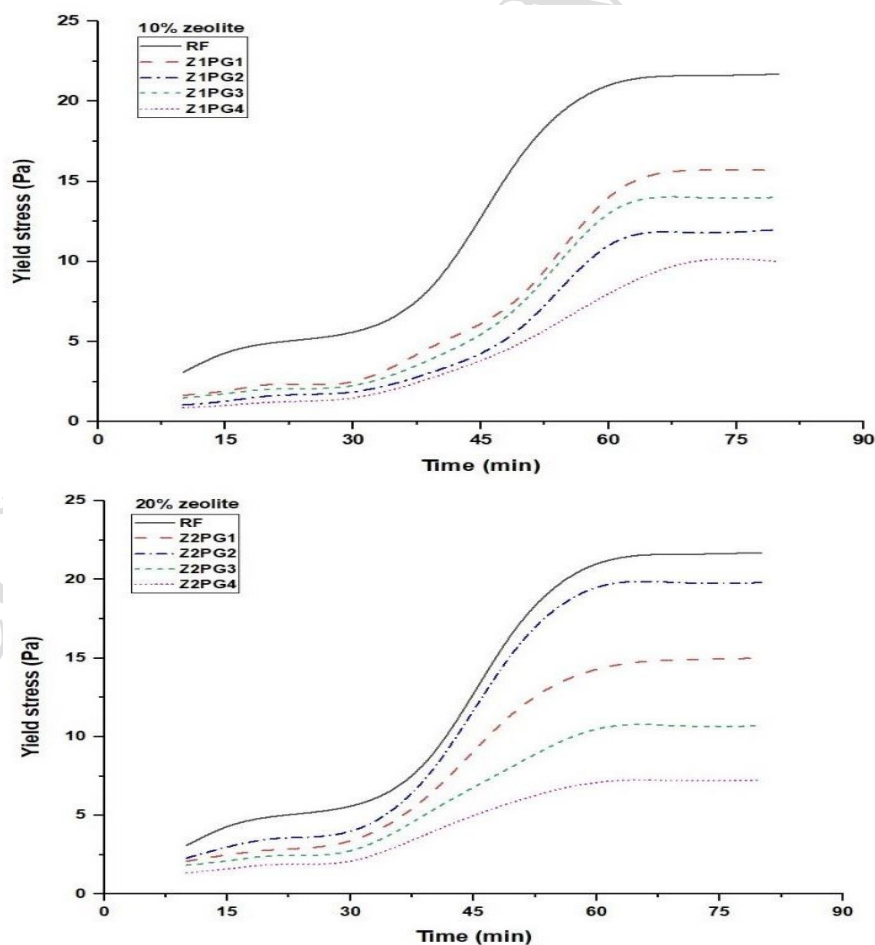


272
273 **Fig. 2 Effects of PG and NZ contents on the slurry fluidity of AAC**

274 Additionally, the fluidity of the AAC mix containing 20% New Zealand wool and the same
275 percentage of PG was reduced by 16.8%. Because of its higher surface area and porous structure,
276 NZ with PG requires more water, significantly reducing its workability. However, the thickening
277 behaviour of the NZ when combined with PG was prolonged, which led to a broader time space for
278 the growth of a greater quantity of gas pores.

279 4.1.2 Yield stress development

280 Figure 3 illustrates the progression of yield stress over time for the AACs examined in a
 281 specific study. It shows that after 60 minutes; the yield stress begins to stabilize. This finding
 282 supports that yield stress measurements were only conducted for 70 minutes in this study, aligning
 283 with the average initial setting time of OPC, which is also 60 minutes. The production of hydration
 284 products caused the yield stress to increase over time for all AACs; however, the rate of increase
 285 varied for each AAC. This variation occurred because, during the initial stages of hydration, the
 286 AAC paste containing 20% PG exhibited the lowest yield stress, followed by 15%, 10%, and 5%
 287 PG, respectively, when 10% NZ was substituted for fly ash. The highest yield stress was in the
 288 AAC paste containing 5% PG. Scientists have found that adding more PG to the AAC commanded
 289 a decrease in yield stress experienced at both 10% and 20% NZ. This is chiefly owing to the
 290 creation of a porous microstructure with a more significant percentage of PG, which absorbs more
 291 water. Because the control AAC has less freely available water, the yield stress of the fresh paste is
 292 increased.
 293



294
 295
 296

Fig. 3 Yield stress vs time of developed AACs

297 4.1.3 Volume Expansion of AAC

298 Fig. 4 depicts the fresh AAC pastes' expansion of volume over time. The increase in total
299 volume during AAC can be divided into four distinct phases: the induction stage, the acceleration
300 stage, the deceleration stage, and the steady-state stage. During the induction period of the aeration
301 process, the fresh paste retains nearly all of its initial volume following the mixing stage. During
302 this time, there has also been very little expansion. The creation of a passivation deposit (made of
303 aluminium oxide) on the exterior of the aluminium particles is what causes the induction period.
304 This layer prevents the gas generation reaction from occurring during the allotted time. At this
305 point, the passivation layer is eroded by hydroxyl radicals, which are created by the reaction of
306 aluminium oxide with water. The second stage is known as the acceleration period, and there has
307 been a notable increase in the volume of the fresh paste. This happens since the paste is under low
308 yield stress, and the aeration process is chemically controlled. The deceleration stage is marked by
309 a reduction in the volume expansion rate, even though the volume of the fresh paste continues to
310 increase. At this stage, the yield stress of the paste rises, leading to reduced aeration. In the final
311 phase, called the steady state, the volume expansion of the fresh paste ceases as the paste continues
312 to stiffen. The duration of each stage in the process is influenced by the fresh paste's rheological
313 properties and the aerating agent's gas production potential over time.

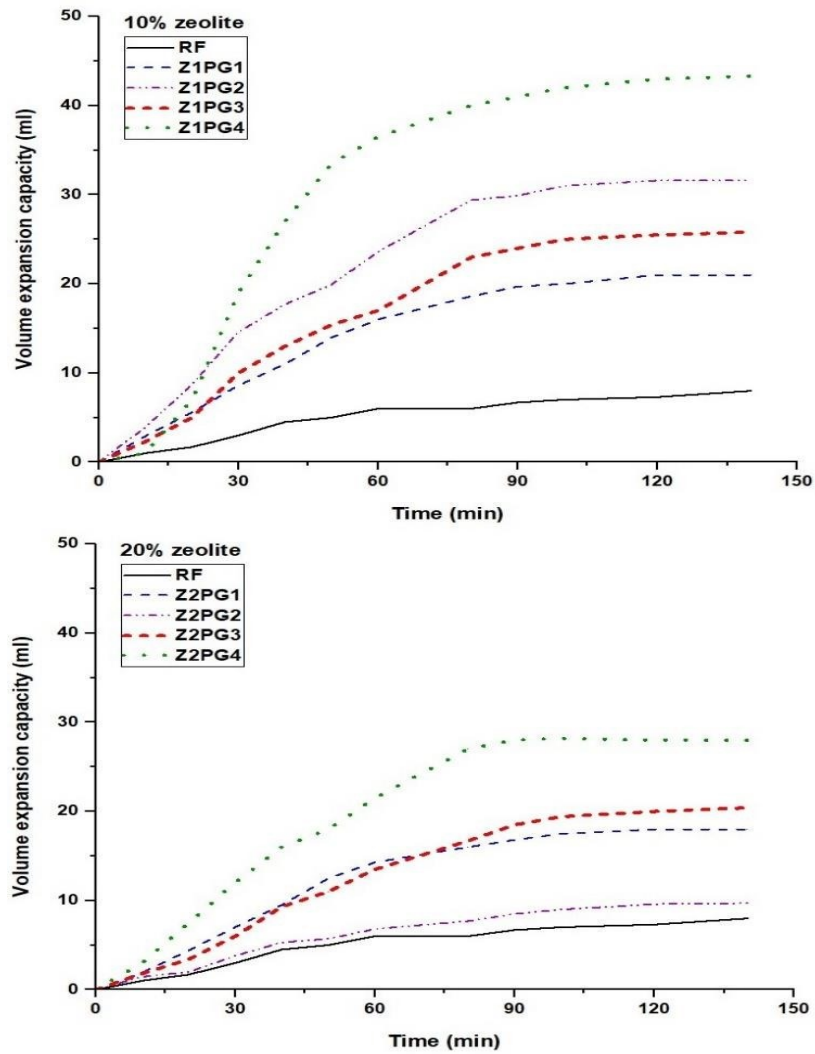


Fig. 4 Volume expansion capacity of developed AACs

314

315

316

317

318

319

320

321

322

323

324

325

326

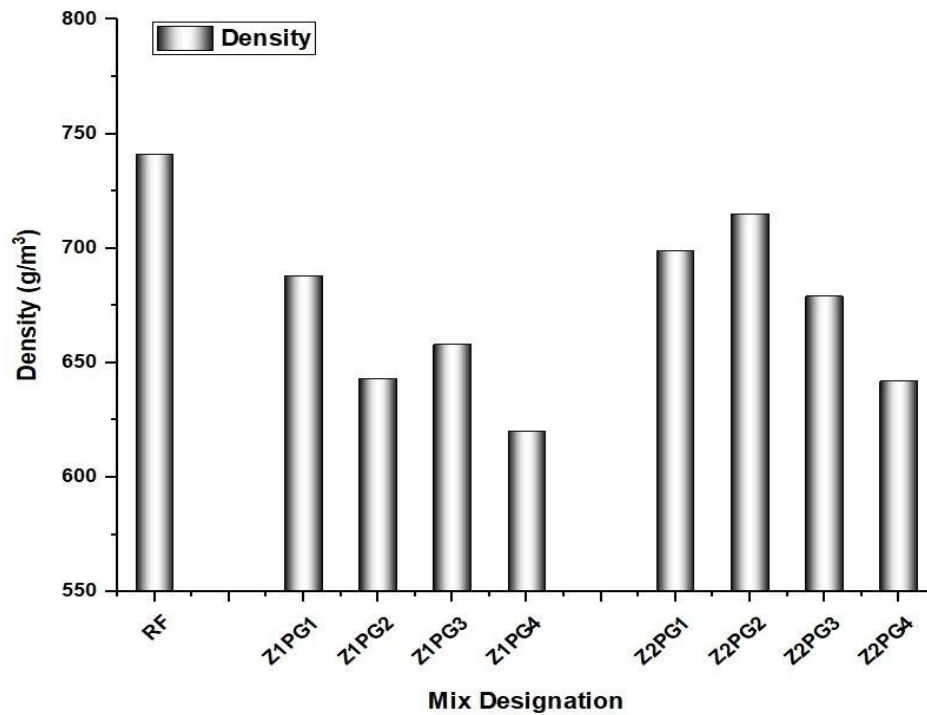
327

328

At the culmination of the 140-minute test, the 20% PG-substituted AAC with 10% and 20% NZ demonstrated the greatest volume expansion of 43 ml and 28 ml, respectively. The control AAC showed a reduced expansion capacity, whereas the PG-replaced AACs displayed a larger expansion than the control. After one hundred minutes, the rate of volume expansion became stable. The volume expansion measurements of the paste are primarily regulated by two key factors: the aerating agent's gas generation potential and the AAC paste's stiffening. The relatively modest volume expansion of the control AAC is likely due to its high yield stress and low gas generation rate. Because of the high dose of PG and the amount of aluminium powder employed as an aerating agent, the yield stress of the AAC paste was significantly reduced, which led to a higher volume expansion. The correct coordination between the two components remains essential to produce an excellent cellular structure in AAC. This is because proper coordination between the two features is also necessary, in addition to the aerating agent's more extensive gas production measurements and the lower yield stress development rate of fresh AAC paste.

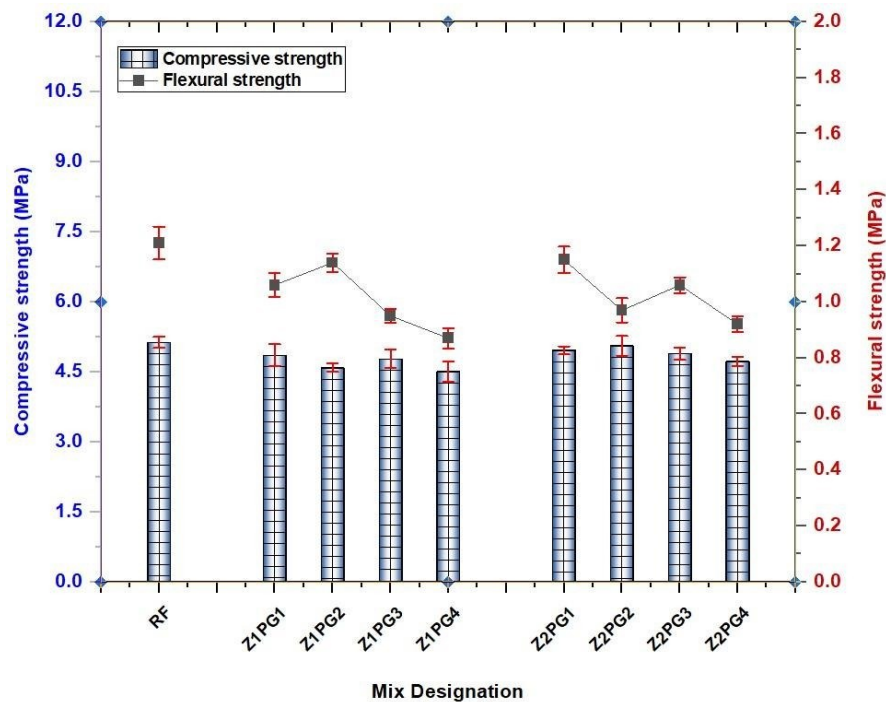
329 **4.2 Effect of PG on AACs strength and density**

330 4.2.1 Density measurements



331 **Fig. 5 Effect of PG on the density of developed AACs**

332 When evaluating the qualities of AAC, bulk density is an essential element that is taken into
333 consideration. Fig. 5 exemplifies by what means the proportions of PG and NZ affect the mixes of
334 AAC concerning their dry densities. The density decreased from 741 g/cm³ to 620 g/cm³ at 10%
335 NZ, while it decreased to 642 g/cm³ at 20% NZ as the percentage of PG replacement increased
336 from 0% to 20%. The density was lowered by approximately 16.3% and 13.4% at 10% and 20%
337 NZ, respectively, once fly ash was replaced with PG equal to 20% of the entire weight. The
338 decrease in density with an increase in PG content can be explained by the formation of AFt and
339 AFm during the pre-curing stage, which leads to a reduction in AAC density. This phenomenon can
340 be detected when the PG concentration of the material is increased. The PG content in the sample
341 significantly impacts the bulk density. The evolution of AFt and AFm has a bigger impact on the
342 developed sample density than the negative effect that PG has on gas foaming. This is because PG
343 harms gas foaming.



345 **Fig. 6 Effect of PG on the strength of developed AACs**

346 As shown in Fig. 6, the compressive strength fell from 5.1 MPa to 4.5 MPa and 5.1 MPa to
 347 4.7 MPa at 10% NZ and 20% NZ, respectively, as the percentage of PG replacement improved
 348 from 0% to 20%. Furthermore, the drop in AAC density can be linked to the compressive strength
 349 loss experienced by the material. It is common knowledge that compressive strength is directly
 350 proportional to bulk density. If the density of AAC is reduced, the material's compressive strength
 351 will often fall as a direct consequence, as this is a general rule. The decrease in compressive
 352 strength can also be partially attributed to the reduction in tobermorite and C-S-H. It is well-known
 353 that the formation of tobermorite and C-S-H under autoclave conditions can contribute to an
 354 increase in the strength of AAC. A higher proportion of PG results in greater gypsum in the AAC
 355 matrix. This, in turn, encourages the development of anhydrite while simultaneously reducing the
 356 development of tobermorite and C-S-H, ultimately reducing strength (Shekarchi et al., 2012).
 357 However, the strength of Z1PG3 improved somewhat when the proportion of RG replacement
 358 grasped 15% at 10% NZ, and a similar modest gain in strength can be perceived at 10% PG
 359 containing AAC (Z2PG2) in the compound. In the succeeding hydrothermal reaction, the synthesis
 360 of tobermorite and the occurrence of an adequate quantity of anhydrite jointly ensure the material's
 361 tensile strength.

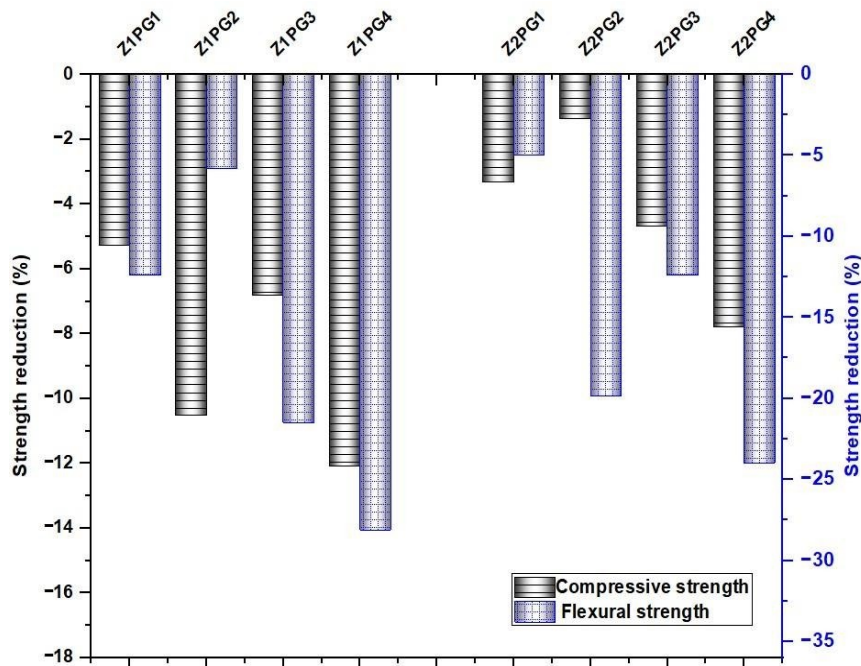


Fig. 7 Strength reduction percentage of developed AACs

363

364

365

366

367

368

369

370

371

372

373

Compared to the control AAC that did not contain additives, the flexural strength was reduced by 28.1% at 10% NZ and 24% at 20% NZ. The result of 1.21 MPa was recorded as the control sample's flexural strength, the highest value obtained. However, the strength values showed a modest rise at particular percentages (10% PG at 10% NZ and 15% PG at 20% NZ), while it's true that the strength values overall had decreased. Compared to the control AAC, the flexural strength revealed a percentage drop of approximately 12.4, 5.8, 21.5, 28.1%, and 5, 19.8, 12.4, and 24.0 at 10 and 20% NZ, respectively. These numbers refer to the reduction in strength at 10 and 20% NZ. The percentages of strength reduction achieved by developed AACs are depicted in Fig. 7.

374

4.3 Gas foaming rate

375

376

377

378

379

380

381

Fig. 8 illustrates the impact of different dosages of PG on slurry behaviour. The control AAC had a pH value of 6.2, which indicates that the acidity level was relatively low. After the PG was added, it should not surprise that the slurry's pH level improved. To be more exact, the rise in the dose of PG from 5% to 20% caused the AAC slurry pH to rise from 7.3 to 9.4 and from 8.1 to 10.6 when the concentration of NZ was either 10% or 20%. Therefore, an efficient method for elevating the pH level of slurry is to combine the incorporation of PG with the employment of natural zeolite.

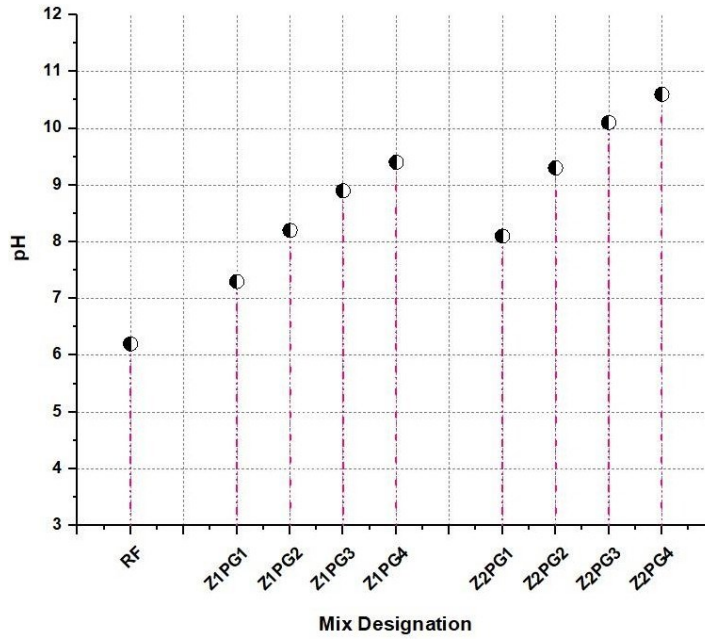


Fig. 8 pH at an early phase of gas foaming

382

383 It is evident from Fig. 9 that the quantity of PG used immediately impacts the volume of
 384 foam produced by the gas, predominantly in the first ten minutes. Within the first ten minutes, the
 385 gas foaming rate decreased as a straight effect of a reduction in the dosage of PG from 20% to 0%.
 386 This can most likely be attributed to the lower alkalinity that results from lowering PG. Due to the
 387 passivation layer already present on the aluminium powder surface, the early foaming response was
 388 stifled. As a result, there was no delay in the onset of the premature gas foaming response in AAC
 389 samples. It is clear that in the nonappearance of any PG component, the development of the slurry
 390 reached over 40 percent in the first 10 minutes. Along with this, the rapid rate of expansion that
 391 occurred during the initial stage also made it easier for the early slurry's strength to expand. Once
 392 the expansion rate of AAC exceeds its setting rate, it can cause hydrogen escape and collapse (Li et
 393 al., 2024). Despite the appropriate foaming of the control AAC in this study, the expansion rate
 394 within 10 minutes indicated significant potential risks in practical engineering applications.

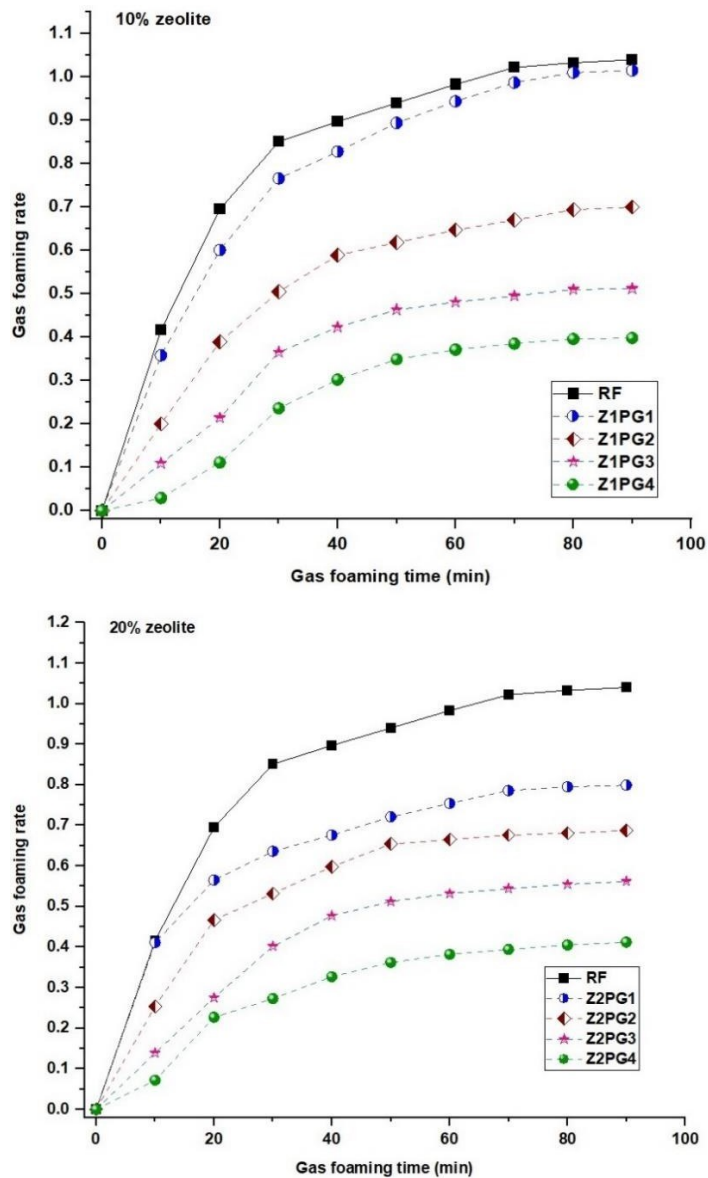


Fig. 9 Gas foaming rate of AACs

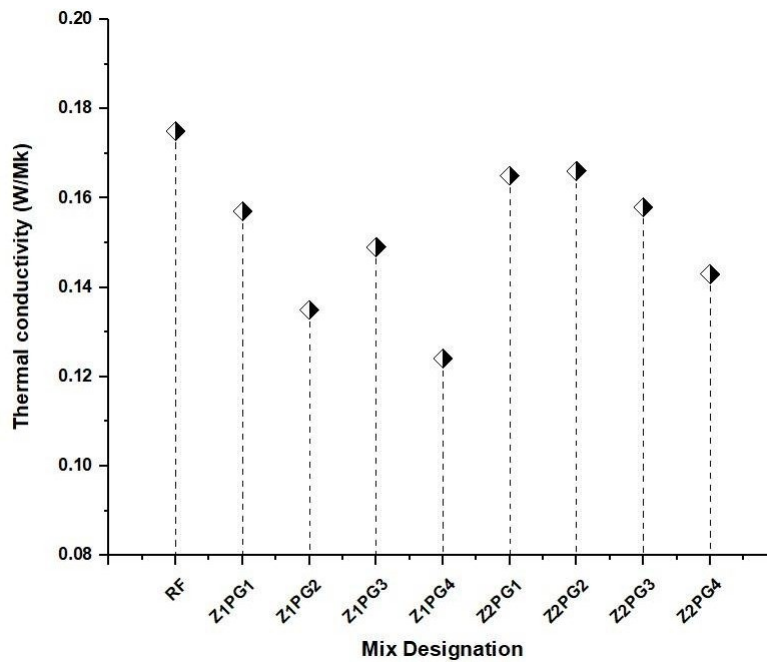
395

396 4.4 Thermal conductivity

397 At a temperature of 194⁰C inside the autoclave, Fig. 10 illustrates the thermal conductivity
 398 measurements of AAC that contain varying amounts of Phospho-Gypsum (PG) and Natural Zeolite
 399 (NZ). It is easy to see a connection between thermal and strength characteristics. In both sets of
 400 research, a growth in the compressive strength commanded towards an increment in the heat
 401 conductivity of the material. However, a modest rise in conductivity values is noticed when the PG
 402 level reaches 15% and 10% in AAC at 10% NZ and 20% NZ, respectively. The control AAC has
 403 the maximum thermal conductivity, and the values declined dramatically as the PG content
 404 increased. This agrees with the findings about the compressive behaviour of the created AACs.

405

406

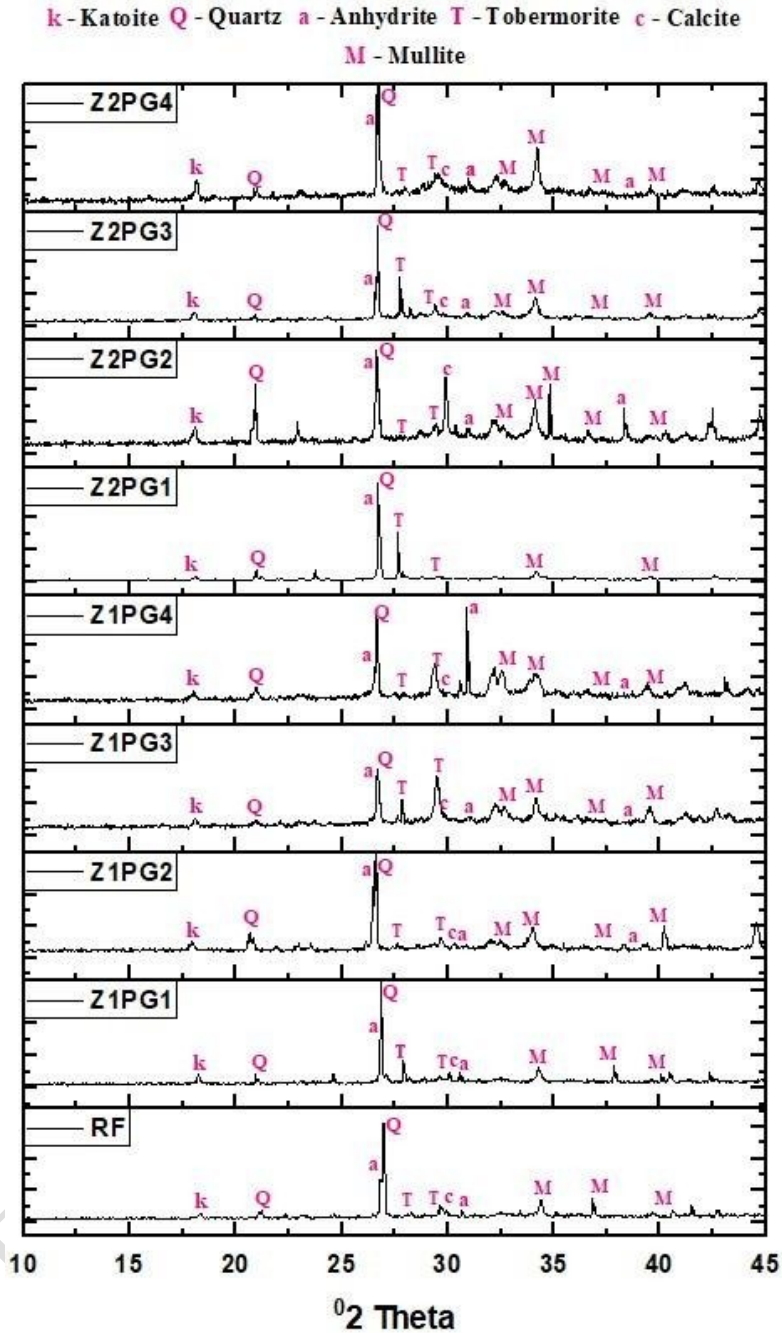


407 **Fig. 10 Effects of PG on the thermal conductivity of AAC**

408 **4.5 XRD analysis**

409 An X-ray diffraction (XRD) analysis was conducted to confirm the phases formed with
 410 different levels of RG present in the AAC. The predominant minerals identified include
 411 tobermorite, mullite, anhydrite, katoite, calcite, and residual quartz, as depicted in Figure 11. The
 412 substitution with PG does not affect the mineral compositions; they are unaltered. On the other
 413 hand, the anhydrite, tobermorite, and katoite concentrations are entirely dissimilar. When PG is
 414 used in place of AAC, there is a considerable alteration in the mineral compositions of each
 415 mineral. Under high pressure and temperature conditions, an increased amount of anhydrite is
 416 produced because of the ongoing increase in PG replacement. As previously noted, an essential
 417 phase of Tobermorite gives AAC samples superior compressive strength while lowering their
 418 density (Sun et al., 2021; Chen et al., 2024). It is abundantly evident that the substitution of PG
 419 does not affect the tobermorite, which serves as the primary result of the reaction. However, a
 420 minor shift matching the complicated structure of tobermorite is observed to occur in the peak
 421 locations of tobermorite when PG-AAC samples are analyzed. This change resulted in a slight shift
 422 in the peak positions of tobermorite. It has been proposed that incorporating waste by-products into
 423 AAC can alter the reaction products.

424

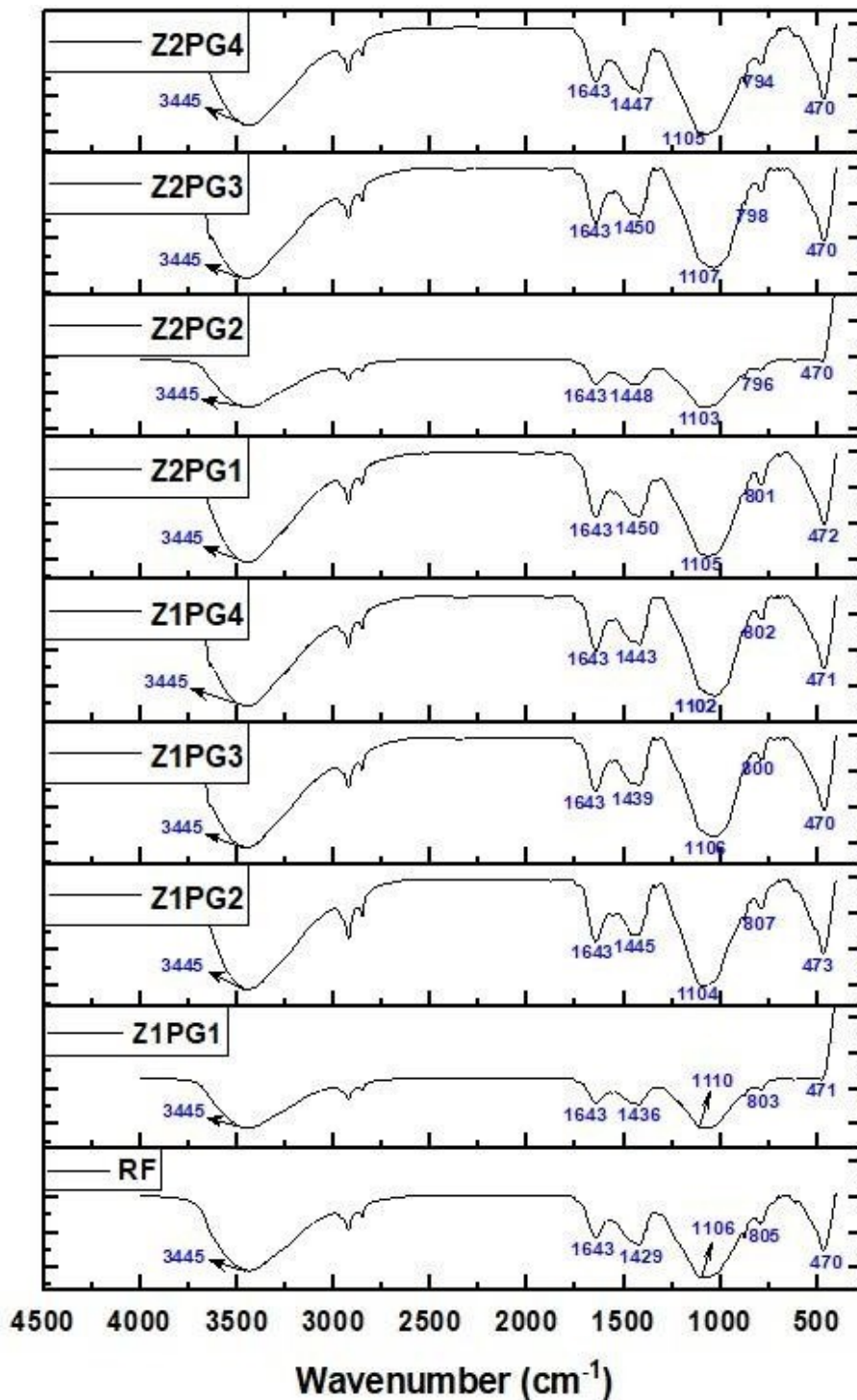


425 **Fig. 11 XRD patterns of developed AACs**

426 **4.6 FTIR analysis**

427 The FTIR spectra of the AAC samples are characterized in Fig. 12. The bending vibration
 428 band of molecule H₂O correlates to the absorption band located approximately 1643 cm⁻¹ in
 429 wavelength. The stretching vibrations of the O-H group are accounted for by the absorption bands
 430 centered at 3445 cm⁻¹ in H₂O, C-S-H, C-H, and tobermorite. The advancement of hydrogen
 431 bonding, which may take on various strengths, is responsible for broadening the band. The peaks
 432 that may be found in the range of 1429 cm⁻¹ to 1450 cm⁻¹ are the asymmetric stretching vibration

433 peaks of CO_3^{2-} , and their presence indicates that calcium carbonate is present in the sample. It is
 434 conceivable that this happened due to the carbonization of CO_2 that grabbed the place throughout
 435 the sample preparation and drying processes. The absorption bands with the greatest strength can be
 436 evident in the region of 1100 cm^{-1} . These bands are associated with the asymmetrical stretching
 437 vibrations of SiO_4 tetrahedra, with peaks at approximately 690, 790, and 807 cm^{-1} corresponding to
 438 the bending vibrations of Si-O-Si. The band at 470 cm^{-1} is attributed to O-Si-O deformation or
 439 bending modes.



440
 441 **Fig. 12 FTIR patterns of developed AACs**

442 **5. Leaching potential and associated risks for each material**

443 **5.1. Natural Zeolite**

444 Natural zeolites are generally considered environmentally friendly; however, they can still
445 leach trace amounts of heavy metals, depending on their source and composition. Studies have
446 shown that while zeolites can absorb pollutants, they may also release certain contaminants under
447 specific conditions, such as acidic environments (Tran et al., 2019). Therefore, careful sourcing and
448 testing are necessary to minimize the risk of leaching.

449 **5.2. Aluminum Powder**

450 Aluminum powder can lead to leaching of aluminum ions, particularly in alkaline
451 environments, which can be toxic to aquatic life if released into water bodies (Mahedi et al., 2019).
452 The leaching potential increases with the particle size and surface area of aluminum powder.
453 Moreover, when aluminum is exposed to moisture, it may undergo oxidation, producing hydrogen
454 gas, which can pose additional safety hazards.

455 **5.3. Phosphogypsum**

456 Phosphogypsum, a by-product of phosphate fertilizer production, has raised significant
457 environmental concerns due to its potential to leach harmful substances, including heavy metals and
458 radioactive elements (Chernysh et al., 2021). Studies have shown that when phosphogypsum is not
459 properly stabilized or contained, it can leach these contaminants into surrounding soils and
460 waterways, posing risks to both human health and the environment.

461 **5.4. Mitigation Strategies**

462 To mitigate the risks of leaching and pollution:

- 463 • **Monitoring and Testing:** Regular leachate testing should be conducted to monitor for heavy
464 metals and other contaminants.
- 465 • **Material Stabilization:** Techniques such as encapsulation and optimizing mix designs can help
466 stabilize contaminants within construction materials.

467 **Controlled Use: Ensuring that materials are sourced from reputable suppliers and are free**
468 **from significant contaminants can also reduce leaching risks.**

469 **6. Limitations and Disadvantages**

470 **6.1 Performance Limitations:**

- 471 • **Mechanical Properties:** While using these materials may enhance certain properties, such as
472 thermal conductivity, they may not achieve the same mechanical strength as conventional
473 concrete components. Research indicates that the incorporation of alternative materials can
474 sometimes lead to a reduction in compressive strength, especially if not optimally blended.

475 • **Durability Issues:** The long-term durability of AAC containing these materials may be a
476 concern. Natural zeolite, while beneficial for some properties, can have varying pozzolanic
477 activity based on its origin, potentially leading to inconsistent performance in different
478 environments.

479 **6.2 Environmental Concerns:**

480 • **Leaching Potential:** As discussed previously, materials like phosphogypsum can leach heavy
481 metals and other contaminants into the environment if not properly managed (Mäkitie et al.,
482 2019). This raises concerns about the sustainability of using such materials in construction, as
483 they may pose risks to both human health and ecosystems.

484 • **Resource Availability:** The availability and sourcing of these materials may also present
485 challenges. For example, while natural zeolite is abundant in some regions, it may not be as
486 readily available in others, leading to increased transportation emissions and costs.

487 **6.3 Economic Considerations:**

488 • **Cost Implications:** The economic feasibility of utilizing these alternative materials can be a
489 significant drawback. Although they may be cheaper than traditional materials in some
490 contexts, processing, transportation, and potential treatment costs associated with leachate
491 management can offset initial savings.

492 • **Market Acceptance:** The construction industry is often slow to adopt new materials due to
493 established standards and practices. Gaining acceptance for AAC incorporating these materials
494 may require extensive testing and validation, which could delay their implementation.

495 **6.4 Regulatory Challenges:**

496 • **Standards and Guidelines:** There may be a lack of established regulatory frameworks
497 governing the use of alternative materials in construction, particularly for by-products like
498 phosphogypsum. This could lead to complications in compliance with building codes and
499 regulations.

500 While the incorporation of natural zeolite, aluminum powder, and phosphogypsum in AAC
501 offers potential benefits, it is essential to consider these limitations and disadvantages in the context
502 of sustainable construction practices. Addressing these concerns will require ongoing research and
503 innovation to optimize material formulations and ensure environmental safety.

504 **Conclusions**

505 The study showed several outcomes that can be summarized as follows:

506 • The incorporation of PG into AAC has the potential to reduce its workability. This could be
507 because PG has a smaller particle size and a greater specific surface area than AAC,
508 meaning it can absorb more water. Due to the slurry's weak fluidity and rapid thickening, it had

509 poor gas generation; as a result, the pores tended to form horizontally and had improved
510 interconnectivity.

- 511 • The yield stress of the control AAC paste was the highest at any given time, followed by
512 rising PG-containing AACs, and then the yield stress was at its lowest for the 20% PG-
513 substituted AAC. Because of its high yield stress and low gas generation rate, control AAC
514 exhibits the most minor volume expansion possible. Because of employing a substantial
515 dosage of PG in conjunction with a proportion of aluminium powder as an aerating agent,
516 the yield stress of the AAC paste was suggestively condensed, which directed to a bigger
517 volume expansion.
- 518 • Using PG in place of fly ash can potentially lessen the density of the sample in both the 10%
519 and 20% NZ substituted AACs. Even if using PG instead of fly ash successfully lowered the
520 rate of gas foaming, the creation of AFt and AFm as a product of this process can cause the
521 density of the sample to drop by a lot.
- 522 • The loss in compressive and flexural strength is attributable to the drop in density of the
523 AAC due to increasing the percentage of PG replacement from 0% to 20% in the material.
524 Growth in the proportion of PG results in a higher proportion of gypsum being present in
525 the AAC reaction matrix; this, in turn, encourages the creation of anhydrite; this, in turn,
526 leads to a lessening in the proportions of tobermorite and C-S-H; and, ultimately, this results
527 in a weaker composite.
- 528 • To be more exact, the value of the AAC slurry's pH rose as the proportion of PG in the
529 mixture climbed from 5% to 20%. The quantity of PG used immediately impacts how much
530 foam the gas produces, particularly in the first ten minutes. In the first ten minutes after the
531 PG dosage was cut from 20% to 0%, there was a drop in the rate at which the gas foamed.
532 The occurrence of the passivation layer on the aluminium powder surface was accountable
533 for preventing an early foaming response from occurring.
- 534 • The AAC made using phosphogypsum exhibited satisfactory strength, density, and thermal
535 conductivity results. The control AAC had maximum thermal conductivity, whereas the
536 values declined dramatically as the PG level increased. However, a modest rise in
537 conductivity values was found when the PG content reached 15% and 10% in AAC at 10%
538 NZ and 20% NZ, respectively.
- 539 • Before autoclaving, C-S-H gels and CH had already been created, and after autoclaving, the
540 majority of the C-S-H gels had been altered into tobermorite. Tobermorite, which is the
541 primary result of the reaction, is not affected in any way by the PG substitution, as can be
542 seen. However, the peak positions of tobermorite are seen to alter ever-so-slightly when PG-
543 AAC samples are analysed, and this shift is seen to correspond to the complicated structure

544 of tobermorite. It has been concluded that including waste by-products in AAC can change
545 the reaction products.

546 **References**

- 547 Ahmed, H., Khan, S., Niazi, M. (2024). "Enhancing the properties of aerated concrete with natural
548 zeolites." *Materials Science Forum*, 1052, 123-132.
549 <https://doi.org/10.4028/www.scientific.net/MSF.1052.123>.
- 550 Ahmed, S., Zhang, W., Liu, H. (2022). "Eco-friendly autoclaved aerated concrete with improved
551 thermal performance." *Journal of Cleaner Production*, 364, 132764.
552 <https://doi.org/10.1016/j.jclepro.2022.132764>.
- 553 Alexa-Stratulat, S. M., Olteanu, I., Toma, A. M., Pastia, C., Banu, O. M., Corbu, O. C., and Toma,
554 I. O. (2023). "The Use of Natural Zeolites in Cement-Based Construction Materials—A State
555 of the Art Review." *Coatings*, 14(1): 18. <https://doi.org/10.3390/coatings14010018>
- 556 Haque, M., B. Chen, Y. Liu, S. Farasat Ali Shah and M. R. Ahmad (2020). "Improvement of
557 physico-mechanical and microstructural properties of magnesium phosphate cement
558 composites comprising with Phosphogypsum." *Journal of Cleaner Production* 261: 121268.
559 <https://doi.org/10.1016/j.jclepro.2020.121268>.
- 560 Arunprathap, K.U., Gokuldeepan P., and Sunilaa George (2022). "Effect of By-product
561 Phosphogypsum in Fly-ash Incorporated Concrete." *International Journal of Creative
562 Research Thoughts (IJCRT)*, 10(7): 67-78. <https://ijcrt.org/papers/IJCRT2207666.pdf>
- 563 I., P. Shafiqh, Z. F. B. Abu Hassan and N. B. Mahyuddin (2018). "Thermal conductivity of
564 concrete – A review." *Journal of Building Engineering* 20: 81-93.
565 <https://doi.org/10.1016/j.jobbe.2018.07.002>.
- 566 ASTM C1693-11 (2017). "Standard Specification for Autoclaved Aerated Concrete (AAC)",
567 American Society of Testing and Materials, USA. <https://doi.org/10.1520/c1693-09e01>.
- 568 ASTM C471M-20 (2024). "Standard Test Methods for Chemical Analysis of Gypsum and
569 Gypsum Products (Metric)", American Society of Testing and Materials, USA,
570 <https://doi.org/10.1520/c0471m-17>.
- 571 Cai, L., X. Li, B. Ma and Y. Lv (2018). "Effect of binding materials on carbide slag based high
572 utilization solid-wastes autoclaved aerated concrete (HUS-AAC): Slurry, physic- mechanical
573 property and hydration products." *Construction and Building Materials* 188: 221-236.
574 <https://doi.org/10.1016/j.conbuildmat.2018.08.115>.
- 575 Campos, M. P., L. J. P. Costa, M. B. Nisti and B. P. Mazzilli (2017). "Phosphogypsum recycling
576 in the building materials industry: assessment of the radon exhalation rate." *Journal of
577 Environmental Radioactivity* 172: 232-236. <https://doi.org/10.1016/j.jenvrad.2017.04.002>.

578 Chen, G., F. Li, P. Jing, J. Geng and Z. Si (2021) "Effect of Pore Structure on Thermal
579 Conductivity and Mechanical Properties of Autoclaved Aerated Concrete." *Materials* 14.
580 <https://doi.org/10.3390/ma14020339>.

581 Chen, W., Yang, F., Xu, Q. (2024). "Utilization of phosphogypsum in building materials: A
582 comprehensive review." *Construction and Building Materials*, 356, 129278.
583 <https://doi.org/10.1016/j.conbuildmat.2023.129278>.

584 Chernysh, Y., Yakhnenko, O., Chubur, V., and Roubík, H. (2021). "Phosphogypsum recycling: a
585 review of environmental issues, current trends, and prospects." *Applied Sciences*, 11(4):
586 1575. <https://doi.org/10.3390/app11041575>

587 Cong, X. Y., S. Lu, Y. Yao and Z. Wang (2016).
588 "Fabrication and characterization of self-ignition coal gangue autoclaved aerated concrete."
589 *Materials & Design* 97: 155-162. <https://doi.org/10.1016/j.matdes.2016.02.068>.

590 El-Didamony, H., A. Amer, M. Mohammed and M. El-Hakim (2019). "Fabrication and properties
591 of autoclaved aerated concrete containing agriculture and industrial solid wastes." *Journal of
592 Building Engineering* 22. <https://doi.org/10.1016/j.jobe.2019.01.023>.

593 Falliano, D., S. Parmigiani, D. Suarez-Riera, G. A. Ferro and L. Restuccia (2022). "Stability,
594 flexural behavior and compressive strength of ultra-lightweight fiber-reinforced foamed
595 concrete with dry density lower than 100 kg/m³." *Journal of Building Engineering* 51:
596 104329. <https://doi.org/10.1016/j.jobe.2022.104329>.

597 González-Torres, M., L. Pérez-Lombard, J. F. Coronel, I. R. Maestre and D. Yan (2022). "A
598 review on buildings energy information: Trends, end-uses, fuels and drivers." *Energy Reports*
599 8: 626-637. <https://doi.org/10.1016/j.egy.2021.11.280>.

600 Guo, X. and T. Zhang (2020). "Utilization of municipal solid waste incineration fly ash to produce
601 autoclaved and modified wall blocks." *Journal of Cleaner Production* 252: 119759.
602 <https://doi.org/10.1016/j.jclepro.2019.119759>.

603 He, J., Q. Gao, X. Song, X. Bu and J. He (2019). "Effect of foaming agent on physical and
604 mechanical properties of alkali-activated slag foamed concrete." *Construction and Building
605 Materials* 226: 280-287. <https://doi.org/10.1016/j.conbuildmat.2019.07.302>.

606 Holanda, F. d. C., H. Schmidt and V. A. Quarcioni (2017). "Influence of phosphorus from
607 phosphogypsum on the initial hydration of Portland cement in the presence of
608 superplasticizers." *Cement and Concrete Composites* 83: 384-393.
609 <https://doi.org/10.1016/j.cemconcomp.2017.07.029>.

610 Huang, F., J. Zhang, X. Zheng, Y. Wu, T. Fu, S. Easa, W. Liu and R. Qiu (2022). "Preparation
611 and performance of autoclaved aerated concrete reinforced by dopamine- modified
612 polyethylene terephthalate waste fibers." *Construction and Building Materials* 348:
128649. DOI: <https://doi.org/10.1016/j.conbuildmat.2022.128649>.

613 IS 12269 (1987). "53 grade ordinary Portland cement", Indian Standards, India.
614 <https://doi.org/10.3403/30304852>.

615 Johnson, R., Hall, D., Wang, M. (2021). "Mechanical behavior of AAC blocks with natural zeolite
616 additives." *Journal of Construction Engineering and Management*, 147(12), 04021195.
617 [https://doi.org/10.1061/\(ASCE\)CO.1943-7862.0002178](https://doi.org/10.1061/(ASCE)CO.1943-7862.0002178).

618 Kadhim, A., M. Sadique, R. Al-Mufti and K. Hashim (2020). "Long-term performance of novel
619 high-calcium one-part alkali-activated cement developed from thermally activated lime kiln
620 dust." *Journal of Building Engineering* 32: 101766.
621 <https://doi.org/10.1016/j.jobe.2020.101766>.

622 Kim, H., J. Hong and S. Pyo (2018). "Acoustic characteristics of sound absorbable high
623 performance concrete." *Applied Acoustics* 138: 171-178.
624 <https://doi.org/10.1016/j.apacoust.2018.04.002>.

625 Koudelka, T., J. Kruis and J. Maděra (2015). "Coupled shrinkage and damage analysis of
626 autoclaved aerated concrete." *Applied Mathematics and Computation* 267: 427-435.
627 <https://doi.org/10.1016/j.amc.2015.02.016>.

628 Kumar, P., Patel, R., Reddy, B. (2024). "Thermal insulation performance of autoclaved aerated
629 concrete with recycled materials." *Energy and Buildings*, 274, 112375.
630 <https://doi.org/10.1016/j.enbuild.2023.112375>.

631 Laad, D. and V. Jatti (2015). "Investigation into the effect of Aluminium powder on Mechanical,
632 Tribological and Electrical properties of Al-ABS composites." *WSEAS Transactions on
633 Applied and Theoretical Mechanics*, E-ISSN: 2224-3429 10: 47-53.

634 Li, M., W. van Keulen, E. Tijs, M. van de Ven and A. Molenaar (2015). "Sound absorption
635 measurement of road surface with in situ technology." *Applied Acoustics* 88: 12-21.
636 <https://doi.org/10.1016/j.apacoust.2014.07.009>.

637 Li, Q., K. Li, W. Ni, S. Zhang, D. Li and W. Chen (2019). "Analysis on Gold Tailings- Based
638 Aerated Concrete in Different Phases of Autoclave Curing Based on Nuclear Magnetic
639 Resonance." *Revue des composites et des matériaux avancés* 29: 381-387.
640 <https://doi.org/10.18280/rcma.290607>.

641 Li, W., Zhang, C., Zhou, X. (2020). "Investigation of AAC with phosphogypsum and natural
642 zeolite." *Journal of Sustainable Cement-Based Materials*, 9(4), 255-272.
643 <https://doi.org/10.1080/21650373.2020.1767742>.

644 Li, X., Zhang, Y., Wang, H., Gao, M. (2024). "Mechanical and thermal properties of zeolite-based
645 autoclaved aerated concrete." *Journal of Building Engineering*, 50, 104587.
646 <https://doi.org/10.1016/j.jobe.2024.104587>.

647 Liu, Y., G. Chen, Z. Wang, Z. Chen, Y. Gao and F. Li (2020) "On the Seismic Performance of

648 Autoclaved Aerated Concrete Self-Insulation Block Walls." *Materials* 13.
649 <https://doi.org/10.3390/ma13132942>.

650 Loginova, E., K. Schollbach, M. Proskurnin and H. J. H. Brouwers (2023). "Mechanical
651 performance and microstructural properties of cement mortars containing MSWI BA as a
652 minor additional constituent." *Case Studies in Construction Materials* 18: e01701.
653 <https://doi.org/10.1016/j.cscm.2022.e01701>.

654 Ma, B.-g., L.-x. Cai, X.-g. Li and S.-w. Jian (2016). "Utilization of Iron Tailings as Substitute in
655 Autoclaved Aerated Concrete: Physico-mechanical and Microstructure of Hydration
656 Products." *Journal of Cleaner Production* 127. <https://doi.org/10.1016/j.jclepro.2016.03.172>.

657 Mahedi, M., Cetin, B., and Dayioglu, A. Y. (2019). "Leaching behavior of aluminum, copper, iron
658 and zinc from cement activated fly ash and slag stabilized soils." *Waste Management*, 95:
659 334-355. <https://doi.org/10.1016/j.wasman.2019.06.018>

660 Miao, C., Wang, H., Liu, X. (2023).
661 "Enhanced mechanical properties of aerated concrete with natural zeolite." *Construction and
662 Building Materials*, 340, 127835. <https://doi.org/10.1016/j.conbuildmat.2023.127835>.

662 Mohammadi, M., Fakharian, P., Nemati, A. (2020). "Influence of natural zeolites on the
663 mechanical properties of AAC." *Journal of Building Engineering*, 32, 101730.
664 <https://doi.org/10.1016/j.jobe.2020.101730>.

665 Murali, G., and Azab, M. (2023). "Recent research in utilization of phosphogypsum as building
666 materials." *Journal of Materials Research and Technology*, 25: 960-987.
667 <https://doi.org/10.1016/j.jmrt.2023.05.272>

668 Nambiar, E., Ramachandran, D., Menon, V. (2023). "Thermal performance of phase change
669 material-coated AAC with recycled content." *Sustainability*, 15(1), 187.
670 <https://doi.org/10.3390/su15010187>.

671 Natarajan, R., Priya, P., Ravikumar, V. (2021). "Recycling of waste materials in AAC: A
672 sustainable approach." *Sustainability*, 13(24), 13927. <https://doi.org/10.3390/su132413927>.

673 Pinilla Melo, J., A. Sepulcre Aguilar and F. Hernández Olivares (2014). "Rheological properties
674 of aerated cement pastes with fly ash, metakaolin and sepiolite additions." *Construction and
675 Building Materials* 65: 566-573. <https://doi.org/10.1016/j.conbuildmat.2014.05.034>.

676 Qian, B., Hu, Y. (2023). "The influence of disused ZSM-5 on the performance of
677 phosphogypsum-based autoclaved aerated concrete." *Buildings*, 13(12), 3012.
678 <https://doi.org/10.3390/buildings13123012>.

679 Qiao, Y., Zhang, H., Wang, R. (2020). "Sustainable construction materials: Phosphogypsum and
680 zeolite in AAC." *Construction and Building Materials*, 243, 118304.
681 <https://doi.org/10.1016/j.conbuildmat.2020.118304>.

682 Qu, X. and X. Zhao (2017). "Previous and present investigations on the components,

683 microstructure and main properties of autoclaved aerated concrete – A review." *Construction*
684 *and Building Materials* 135: 505-516. <https://doi.org/10.1016/j.conbuildmat.2016.12.208>.

685 Rahman, R. A., Fazlizan, A., Asim, N., and Thongtha, A. (2021). "A review on the utilization of
686 waste material for autoclaved aerated concrete production." *Journal of Renewable*
687 *Materials*, 9(1): 61-72. <https://doi.org/10.32604/jrm.2021.013296>

688 Rashad, A. M. (2017). "Phosphogypsum as a construction material." *Journal of Cleaner*
689 *Production* 166: 732-743. <https://doi.org/10.1016/j.jclepro.2017.08.049>.

690 Reddy, B. V., Prasad, D., Gupta, A. (2022). "Utilizing waste materials in the production of
691 autoclaved aerated concrete." *Journal of Building Engineering*, 45, 103509.
692 <https://doi.org/10.1016/j.jobbe.2022.103509>.

693 Revilla-Cuesta, V., F. Faleschini, M. A. Zanini, M. Skaf and V. Ortega-López (2021). "Porosity-
694 based models for estimating the mechanical properties of self-compacting concrete with
695 coarse and fine recycled concrete aggregate." *Journal of Building Engineering* 44: 103425.
696 <https://doi.org/10.1016/j.jobbe.2021.103425>.

697 Rosales, J., S. M. Pérez, M. Cabrera, M. J. Gázquez, J. P. Bolivar, J. de Brito and F. Agrela
698 (2020). "Treated phosphogypsum as an alternative set regulator and mineral addition in
699 cement production." *Journal of Cleaner Production* 244: 118752.
700 <https://doi.org/10.1016/j.jclepro.2019.118752>.

701 Shekarchi, M., Ahmadi, B., and Najimi, M. (2012). "Use of natural zeolite as pozzolanic material
702 in cement and concrete composites." Chapter, 27, 665-694.
703 <https://doi.org/10.2174/978160805261511201010665>

704 Shekarchi, M., Ahmadi, B., Azarhomayun, F., Shafei, B., and Kioumars, M. (2023). "Natural
705 zeolite as a supplementary cementitious material—A holistic review of main properties and
706 applications." *Construction and Building Materials*, 409: 133766.
707 <https://doi.org/10.1016/j.conbuildmat.2023.133766>

708 Schreiner, J., D. Jansen, D. Ectors, F. Goetz-Neunhoeffler, J. Neubauer and S. Volkmann (2018).
709 "New analytical possibilities for monitoring the phase development during the production of
710 autoclaved aerated concrete." *Cement and Concrete Research* 107: 247-252.
711 <https://doi.org/10.1016/j.cemconres.2018.02.028>.

712 Seddighi, F., G. Pachideh and S. B. Salimbahrami (2021). "A study of mechanical and
713 microstructures properties of autoclaved aerated concrete containing nano-graphene." *Journal*
714 *of Building Engineering* 43: 103106. <https://doi.org/10.1016/j.jobbe.2021.103106>.

715 Serhat Baspinar, M., I. Demir, E. Kahraman and G. Gorhan (2014). "Utilization potential of fly
716 ash together with silica fume in autoclaved aerated concrete production." *KSCE Journal of*
717 *Civil Engineering* 18(1): 47-52. <https://doi.org/10.1007/s12205-014-0392-7>.

718 Singh, K., Kumar, A., Gupta, R. (2020). "Thermal and mechanical analysis of AAC with waste
719 by-products." *Journal of Cleaner Production*, 273, 122923.
720 <https://doi.org/10.1016/j.jclepro.2020.122923>.

721 Suchorab, Z., D. Barnat-Hunek, M. Franus and G. Łagód (2016) "Mechanical and Physical
722 Properties of Hydrophobized Lightweight Aggregate Concrete with Sewage Sludge."
723 *Materials* 9. <https://doi.org/10.3390/ma9050317>.

724 Sun, Y., Li, X., Zhang, H. (2021). "Thermal and mechanical properties of zeolite-phosphogypsum
725 aerated concrete." *Construction and Building Materials*, 307, 124945.
726 <https://doi.org/10.1016/j.conbuildmat.2021.124945>.

727 Tian, T., Y. Yan, Z. Hu, Y. Xu, Y. Chen and J. Shi (2016). "Utilization of original
728 phosphogypsum for the preparation of foam concrete." *Construction and Building Materials*
729 115: 143-152. <https://doi.org/10.1016/j.conbuildmat.2016.04.028>.

730 Tran, Y. T., Lee, J., Kumar, P., Kim, K. H., and Lee, S. S. (2019). "Natural zeolite and its
731 application in concrete composite production." *Composites Part B: Engineering*, 165: 354-
732 364. <https://doi.org/10.1016/j.compositesb.2018.12.084>

733 Trindade, A. D., G. B. A. Coelho and F. M. A. Henriques (2021). "Influence of the climatic
734 conditions on the hygrothermal performance of autoclaved aerated concrete masonry walls"
735 *Journal of Building Engineering* 33:101578. <https://doi.org/10.1016/j.jobe.2020.101578>.

736 Walczak, P., P. Szymański and A. Różycka (2015). "Autoclaved Aerated Concrete based on Fly
737 Ash in Density 350kg/m³ as an Environmentally Friendly Material for Energy – Efficient
738 Constructions." *Procedia Engineering* 122:39-46.
739 <https://doi.org/10.1016/j.proeng.2015.10.005>.

740 Wang, Y., W. Wang, D. Wang, Y. Liu and J. Liu (2021). "Study on the influence of sample size
741 and test conditions on the capillary water absorption coefficient of porous building materials."
742 *Journal of Building Engineering* 43: 103120. <https://doi.org/10.1016/j.jobe.2021.103120>.

743 Wang, J., Li, S., Zhou, Y. (2023). "Optimization of phosphogypsum and zeolite mixtures in
744 aerated concrete." *Journal of Cleaner Production*, 398, 136445.
745 <https://doi.org/10.1016/j.jclepro.2023.136445>.

746 Xu, C., M. L. Nehdi, K. Wang and Y. Guo (2021). "Experimental study on seismic behavior of
747 novel AAC prefabricated panel walls." *Journal of Building Engineering* 44: 103390.
748 <https://doi.org/10.1016/j.jobe.2021.103390>.

749 Yang, S., X. Yao, J. Li, X. Wang, C. Zhang, S. Wu, K. Wang and W. Wang (2021). "Preparation
750 and properties of ready-to-use low-density foamed concrete derived from industrial solid
751 wastes." *Construction and Building Materials* 287: 122946.
752 <https://doi.org/10.1016/j.conbuildmat.2021.122946>.

- 753 Yuan, B., C. Straub, S. Segers, Q. L. Yu and H. J. H. Brouwers (2017). "Sodium carbonate
754 activated slag as cement replacement in autoclaved aerated concrete." *Ceramics International*
755 43(8): 6039-6047. <https://doi.org/10.1016/j.ceramint.2017.01.144>.
- 756 Zhai, S., P. Zhang, Y. Xian, J. Zeng and B. Shi (2018). "Effective thermal conductivity of
757 polymer composites: Theoretical models and simulation models." *International Journal of*
758 *Heat and Mass Transfer* 117: 358-374.
759 <https://doi.org/10.1016/j.ijheatmasstransfer.2017.09.067>.
- 760 Zhang, X., Liu, Y., Wang, J. (2022). "Thermal insulation properties of AAC incorporating
761 industrial by-products." *Construction and Building Materials*, 330, 127252.
762 <https://doi.org/10.1016/j.conbuildmat.2022.127252>.
- 763 Zhang, Y., S. Zhang, W. Zhao, X. Jiang, Y. Chen, J. Hou, Y. Wang, Z. Yan and H. Zhu (2023).
764 "Influence of multi-scale fiber on residual compressive properties of a novel rubberized
765 concrete subjected to elevated temperatures." *Journal of Building Engineering* 65: 105750.
766 <https://doi.org/10.1016/j.jobbe.2022.105750>.
- 767 Zhao, F., Li, X., Zhang, Z. (2020). "Optimization of autoclaved aerated concrete mixtures with
768 natural zeolites." *Materials Science and Engineering: A*, 788, 139574.
769 <https://doi.org/10.1016/j.msea.2020.139574>.
- 770 Zhao, X., Zhang, L., Chen, H. (2023). "Sustainable use of industrial waste in construction
771 materials: A review." *Resources, Conservation and Recycling*, 190, 106735.
772 <https://doi.org/10.1016/j.resconrec.2023.106735>.